

SLAC-PUB-7748
UMS/HEP/97/009
January 1998

The CsI(Tl) Calorimeter of the BABAR Detector*

Johannes M. Bauer
Department of Physics
University of Mississippi
University, MS 38677, USA

Representing the BABAR Calorimeter Group[†]

Stanford Linear Accelerator Center
Stanford University
Stanford, CA 94309, USA

Abstract

The Asymmetric B-Factor at the Stanford Linear Accelerator Center will study the $B\text{-}\bar{B}$ meson system with focus on CP violation. Its detector BABAR contains a high-resolution CsI(Tl) calorimeter, which is currently under construction. The final design of the calorimeter (from the crystals to the calibration system) will be presented in this report.

Invited talk presented at the
7th International Conference on Calorimetry
in High-Energy Physics (ICCHEP 97)
Tucson, Arizona, USA
November 9–14, 1997

*Work supported in part by Department of Energy contract DE-AC03-76SF00515.

1 The Asymmetric B-Factory: Overview and Requirements

In early 1999, the Asymmetric B-Factory at the Stanford Linear Accelerator Center (SLAC) is scheduled to start its operation. Electrons and positrons will be accelerated in the SLAC linear accelerator to 9.0 GeV and 3.1 GeV, respectively, and stored in the PEP-II ring which is located at the eastern end of the accelerator. The choice of beam energies corresponds to the $\Upsilon(4S)$ resonance at an energy of 10.6 GeV. In the BABAR detector,¹ beam crossings will occur every 4.2 ns. The final luminosity is expected to be $10^{34} \text{ cm}^{-2}\text{s}^{-1}$, generating about ten $B^0\overline{B}^0$ events every second at the $\Upsilon(4S)$ resonance.

With the boost due to the asymmetric energies, the two B -vertices and their decay sequence may be more easily distinguished than is possible in colliders with equal energies for electrons and positrons. The BABAR detector has to provide good momentum and energy resolution and particle identification, as well as precise information about the vertices, and has to cover a large solid angle.

2 The Design of the BABAR Calorimeter

2.1 Expected Resolution

Decays important for CP violation studies are, for example, $B^0 \rightarrow \rho^\pm \pi^\pm$ with $\rho^\pm \rightarrow \pi^\pm \pi^0$, or $B^0 \rightarrow J/\psi K_s^0 \rightarrow e^+ e^- \pi^+ \pi^-$. Generic B decays create in the average about 5.5 photons with about half of the photons having energies less than 200 MeV, while photons of the channel $B^0 \rightarrow \pi^0 \pi^0$ may reach energies up to 4.5 GeV. Good resolution and efficiency for detecting the photons from pion decay is therefore important for the reconstruction of the events. The calorimeter is designed to resolve the energy and angular position of photons very well from 5 GeV down to 20 MeV. The goal for the energy resolution is

$$\frac{\sigma_E}{E} = \frac{1\%}{\sqrt[4]{E(\text{GeV})}} \oplus 1.2\% \quad (1)$$

for photons at an angle of 90° . The constant term contains the errors from transverse and longitudinal leakage, calibration, and non-uniformities in the light yield.

The angular resolution is expected to be

$$\sigma_\theta = \frac{3 \text{ mr}}{\sqrt{E(\text{GeV})}} \oplus 2 \text{ mr}. \quad (2)$$

The electronic noise is required to have an equivalent noise energy (ENE) $\leq 150 \text{ keV}$ or less to allow good energy resolution at low energies.

The solid angle coverage is approximately symmetric in the center-of-mass frame with $|\cos\theta_{cm}| < 0.91$. In the laboratory frame, the coverage is from 140° to 26.6° for the barrel, and extends down to 15° with the endcap.

2.2 Properties of CsI(Tl)

The calorimeter is surrounded by a 1.5 T magnetic field. This design choice as well as space and cost constraints led to the decision to use CsI(Tl) as material for the calorimeter and photodiodes for the readout. CsI(Tl) has a high light yield ($50 - 60 \times 10^3$ photons/MeV) and is suitably stable under radiation. The radiation dose at PEP-II is expected to be around 1.5 krad/yr at a distance of 0.45 m from the beam line, and 0.5 krad/yr at a distance of 1 m from the beam line.

The concentration of thallium iodide in the crystals is usually around 500 ppm. The radiation length of CsI(Tl) is $X_0 = 18.6$ mm, the absorption length is 342 mm, and the decay time is relatively slow at 940 ns. The crystals are slightly hygroscopic and have to be stored at very low humidity, but they still can be handled for several days at about 40% humidity without loss in quality.

2.3 Crystal Arrangement and Quality Control

The barrel calorimeter contains 48 different crystal types. 120 crystals of each type form a ring around the beam axis. This leads to a total of 5760 crystals in the barrel calorimeter. The crystals are chosen to be up to $17.5 X_0$ in length to limit leakage and to therefore allow for good resolution. The length of the barrel crystals ranges from 297.6 mm ($16 X_0$) to 325.5 mm ($17.5 X_0$). The endcap has 820 crystals of eight different types with lengths of 17 or $17.5 X_0$.

Each crystal has a trapezoidal shape and has to be machined precisely up to $\pm 150 \mu\text{m}$ tolerance. Upon delivery from the vendors, the quality control procedure checks the dimensions and, using a phototube and collimated ^{22}Na source, the light yield. The light yield is required to be high enough overall, but also has to be uniform along the length of the crystal: For the first 12 cm, the light yield may not vary by more than 2% from the average. Further along, the uniformity limit is relaxed linearly towards the end of the crystal, where the light yield may vary by up to 6% at a distance of 35 cm from the front.

The crystals are wrapped into two layers of Tyvek of $160 \mu\text{m}$ thickness (diffuse reflective and robust material), one layer of aluminum foil ($25 \mu\text{m}$ thick), and one layer of mylar ($13 \mu\text{m}$ thick, insulator between aluminum foil and carbon fiber housing).

2.4 Photodiodes

The scintillating light is collected by photodiodes of type Hamamatsu S 2744-08 silicon PIN, each with an active area of $1 \times 2 \text{ cm}^2$. They have a quantum efficiency of 84% at the peak light emission for CsI(Tl) of 550 nm. Two diodes (for redundancy) are mounted at the back of each crystal, with a transparent polystyrene plate separating the crystal from the diode, joined together with epoxy.

Since the bond to the crystal is weaker than the bond to the diode, a special test was performed to study the strength of the former bond under temperature variations. A plate of polystyrene was glued onto 127 slices of CsI(Tl). The samples were placed in a temperature controlled box, and the temperature was cycled 158 times by ± 4 and $\pm 5^\circ\text{C}$ with each cycle lasting about eight hours. This corresponds to cycling all crystals of the calorimeter three times. The light yield of the samples was measured five times, once at the beginning of the test, and four times later. The light yields were normalized so that the mean of the first measurement was 100%. The results can be seen in Figure 1. No significant change in the mean of the light yield was observed over the duration of the test. Also, no single sample showed a sharp drop in light yield which could indicate a separation of the epoxy from either the crystal or the polystyrene.

After gluing the diodes to the crystals, the light yield of each crystal is measured with an ^{88}Y source placed at the front end of the crystal. Via calibration with an ^{241}Am source, the output of the photodiodes can be given in terms of photoelectrons per MeV. Results from more than 4000 crystals are shown in Figure 2. The light yield of the crystals ranges from about 5000 to about 10000 e^-/MeV , with the mean at around 7500 e^-/MeV . Considering that the equivalent noise current in each diode is about 600 e^- , the equivalent noise energy (ENE) for the mean is around 115 keV per crystal.

2.5 Pre-Amplifier

The photodiodes are connected to pre-amplifiers which are housed right behind the crystals in a small aluminum frame, covered with a lid. A dynamic range of 18 bits is achieved as follows: For each photodiode, the pre-amplifier provides two output signals with a gain ratio of 32. From the pre-amplifier, the signals travel to ADC boards at the ends of the detector. Here the signals are again amplified with two different gains. Then the signals from the two photodiodes are added. The signal with the most appropriate gain is sent to a 10-bit ADC. Together with two bits indicating the range, the signal is then passed on to the trigger electronics.

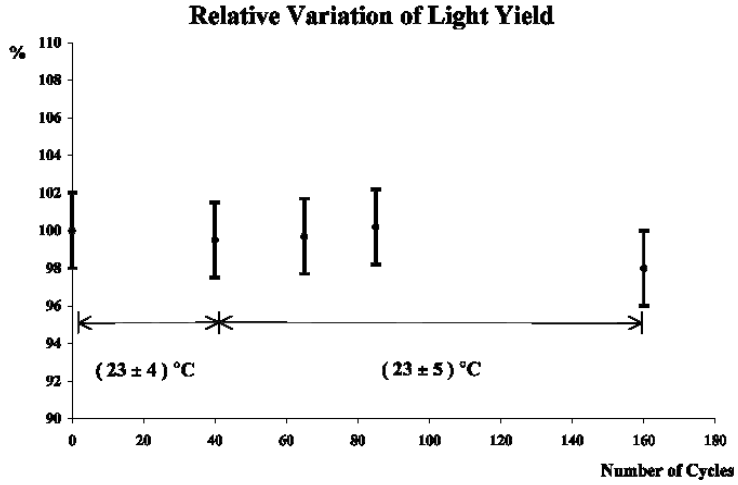


Figure 1: Results from a test to study the reliability of the glue joint between the crystal and polystyrene surface. The measurements were normalized to have an initial mean of 100%. No significant drop in light yield was observed when the temperature of the samples was varied by ± 4 and $\pm 5^\circ\text{C}$.

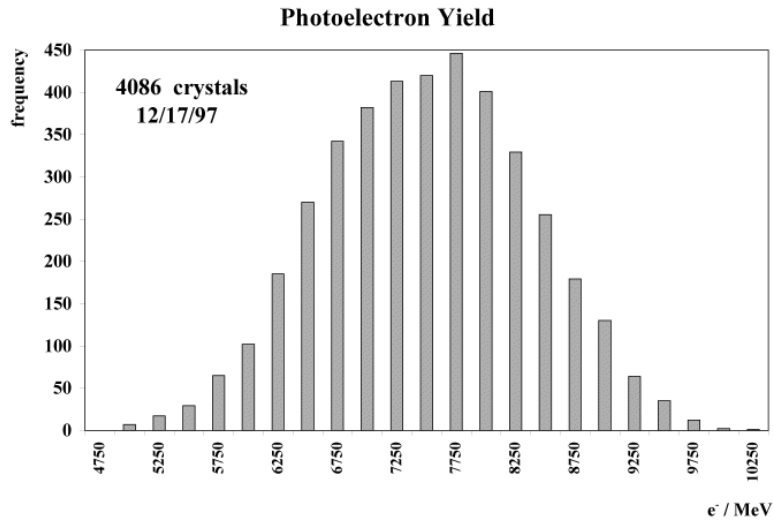


Figure 2: Histogram of the light yield in photoelectrons/MeV measured for more than 4000 crystals. The measurements were performed after the photodiodes were glued to the crystals.

2.6 Modules and Installation

Once the diodes are glued to the crystals, they are assembled into “modules.” In total, the barrel is segmented into 280 modules of seven different types. Each type forms a ϕ -ring out of 40 modules (surrounding the beam line). Four module types form the forward half of the barrel, three the backward half. Each module contains 21 crystals (three crystals each from seven different crystal types). The backward-most modules are an exception, containing 18 crystals (three crystals each from six crystal types). The endcap has 20 identical modules with 41 crystals each.

In both the barrel and endcap, the crystals are projectively pointing towards the interaction point. Only along the angle θ_{lab} , the crystals are slightly non-projective ($\theta_{\text{lab}} = 90^\circ$ if perpendicular to beam line). Here the planes with the inactive material between the crystals do not point straight to the interaction point, but instead are slightly tilted.

The module housings for both the barrel and the endcap are made of carbon fiber (CF), molded from mandrels in the shape of crystals and troughs which determine the outside dimensions of the carbon fiber housing. Around each mandrel, a CF layer of $330\ \mu\text{m}$ thickness is placed, while a $200\ \mu\text{m}$ thick CF layer is placed at the outside. After allowing the epoxy to cure, the wall thickness of the CF housing is about 0.7 mm between crystals and about 0.55 mm at the outside walls.

Once the crystals are inserted into the CF housing and glued into place, an aluminum “strong back” is fixed to the back of the housing. Via the strong back, the module will be aligned at the inside of the “strong support cylinder,” a large cylindrical aluminum structure. The weight of the modules will therefore only be supported via the aluminum strong backs by the strong support cylinder, not by neighboring modules. No additional material will have to be placed in front of the crystals, and better physics performance can be achieved. Numerous openings in the cylinder allow access to cables and electronics during the installation of the modules. The inner radius of the completed barrel will be 0.9 m, the outer radius 1.36 m. The length will be about 3 m.

Like the barrel, the endcap modules will be held via aluminum strong backs. They will be installed on two C-shaped frames, which can be moved sideways and back to allow easy access during down-time.

3 Calibration and Monitoring Systems

The BABAR calorimeter will be calibrated by three different methods: Bhabha scattering and similar physics data, electronic charge injection, and a circulat-

ing radioactive source.^{2,3} A light pulser system³ will monitor the calibration on short time frames. This report will only discuss the rather unique circulating radioactive source in greater detail.

3.1 Bhabha Scattering and Other Physics Data

Enough Bhabha scattering data will be collected in less than one day to allow the calibration of the calorimeter for high energies. Additional channels for calibration, like $e^+e^- \rightarrow \mu^+\mu^-$, need more time to accumulate enough statistics. Calibration of the calorimeter with data, however, cannot be done right from the beginning, but requires the calorimeter response to already be reasonably well understood by other means.

3.2 Light Pulser System for Monitoring Calibration

Light from Xenon flash lamps will be distributed via light fibers to each crystal in the endcap and the barrel. By comparing the response of the crystals to the light from the same Xenon lamp, relative changes of up to 0.5% between the crystals may be detected (0.1% for crystals within one single module).

A reference system will monitor the output of the Xenon flash lamp to allow comparisons between measurements performed at different times. A precision of up to 1% over the period of one week is expected.

3.3 Circulating Radioactive Source

The circulating radioactive source will perform absolute calibrations of the crystals and the readout system at low energy. This is especially valuable at the beginning of the detector life. It will also monitor long-term changes in the system. For example, the light yield might decrease due to radiation damage or due to changes in the optical coupling or wrapping.

The system takes advantage of the radioactive decay chain $^{19}\text{F} + n \rightarrow ^{16}\text{N} + \alpha$. The half-life of ^{16}N is 7 seconds. With a 69% probability, it decays via an excited state into ^{16}O by emitting a 6.13 MeV photon. This photon can be detected in the calorimeter and used for calibration. A typical spectrum is shown in Figure 3. It was obtained in a test with a crystal and acquisition system similar to the ones in the final calorimeter. The 6.13 MeV peak can clearly be seen above the two escape peaks.

For the system to be installed in the BABAR detector, 14 MeV neutrons will be provided by a deuterium-tritium neutron generator with a continuous flux of 10^9 neutrons per second. The generator will be surrounded by a bath filled with fluorinert, FC-77, a non-toxic and chemically inert liquid with a

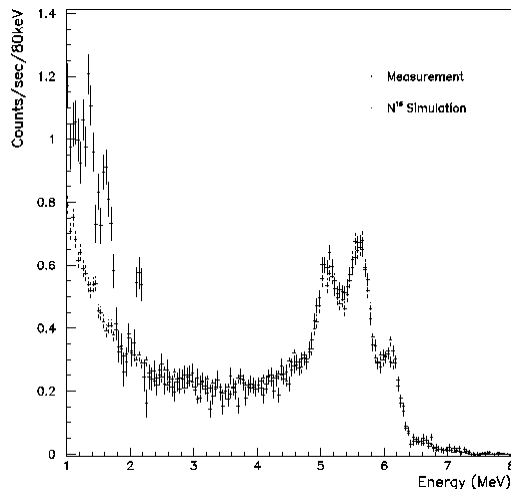


Figure 3: Spectrum from test set-up similar to the calorimeter arrangement. The 6.13 MeV photon peak can clearly be seen next to two escape peaks. Above about 2 MeV, the measurement agrees very well with the simulation.

high content of fluorine and a low viscosity. In case of a spill, it will evaporate from CsI crystals without leaving any residue. Due to the short radioactive life-time of ^{16}N and the ability to turn the neutron generator on and off on demand, the radioactivity in the system can be restricted to the time in which data will be taken.

From the bath, the liquid will be pumped into tubes located in front of both the barrel and the endcap crystals. These tubes will be aluminum tubes of 3/8 inch (9.5 mm) diameter and 0.020 inch walls pressed flat to a height of 5 mm. To increase the mechanical stability, they will be placed between two 0.5 mm thick aluminum sheets (Figure 4). Eight such panels, each covering 45° , will be installed in front of the barrel crystals. The panels will be inserted in the detector between the barrel calorimeter and the DIRC (Detector of Internally Reflected Čerenkov radiation), a particle identification system located radially inward of the barrel calorimeter. At the time of the panel installation, both the barrel calorimeter and the DIRC will have been installed, leaving an overall envelope of only 10 to maximal 15 mm radially for the calibration source panels. Similar tubes will be located in front of the endcap crystals. A schematic drawing with front, side, and rear views can be seen in Figure 5.

About 3.5 liters of fluorinert will be pumped every second through the system with a pressure differential of about 15 psi and a total pressure of

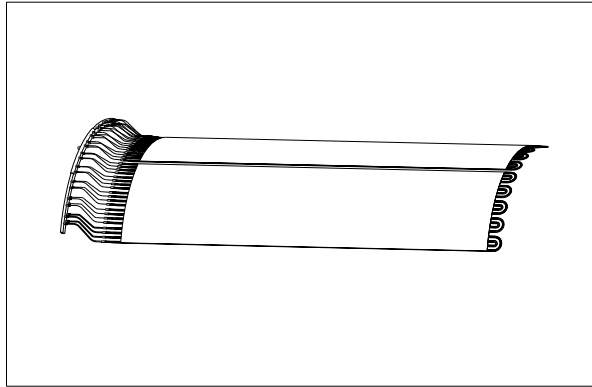


Figure 4: Schematic drawing of two of the eight panels. They contain flattened aluminum tubes through which radioactive fluorinert will circulate in front of the barrel crystals. The liquid enters and exits through the manifold shown on the left side.

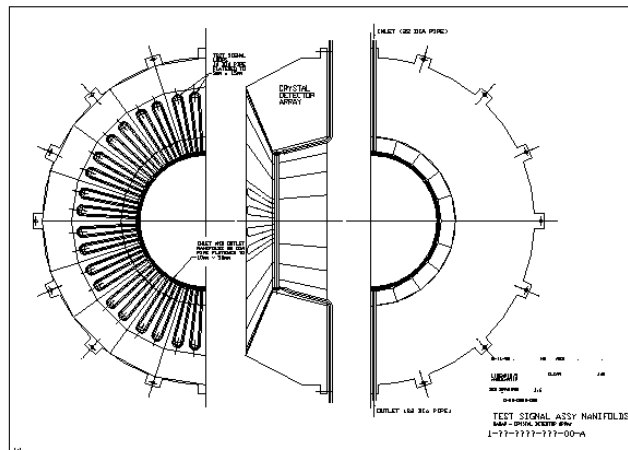


Figure 5: The location of the aluminum tubes through which radioactive fluorinert flows to the endcap crystals is shown in this plot with views from the front, the side, and the rear. Only one half of the endcap is depicted. The aluminum tubes can be recognized by their “hair-pin” shape. They are fed from tubes running from the back through the inner hole of the endcap.

about 30 psi. The fluid will remain in the tubes during normal data-taking at BABAR when the calibration system is not in use, since it only adds little in radiation lengths to the material in front of the crystals.

Runs are scheduled to take about 15 minutes, each collecting around 2700 events per crystal. The design goal is a calibration precision of about 0.25% for a per-crystal noise of 150 keV.

4 Conclusion

At the time of the writing of this report, the BABAR calorimeter is nearing completion. The BABAR calorimeter is designed to reach high resolution and efficiency for photons in a wide range of energies, down to an energy of 20 MeV, with a large solid angle coverage. A unique calibration system with a fluid activated by a neutron generator which delivers low-energy photons to the front of each crystal will be of value for initial calibrations at low energy and for long-term monitoring of the calorimeter.

Acknowledgments

The author wishes to thank his colleagues from the BABAR calorimeter group, in which it is a pleasure to work, as well as the organizers of CALOR 97 for all their work to ensure such a successful conference.

References

- [[†]] The following institutions are involved in the construction of the BABAR Calorimeter: Beijing Glass Research Institute; Ruhr-Universität Bochum; University of Bristol; Brunel University; Budker Institute of Nuclear Physics; California Institute of Technology; University of California, IIRPA; University of California, Irvine; University of Colorado; Technische Universität Dresden; University of Edinburgh; Iowa State University; University of Iowa; Lawrence Livermore National Laboratory; University of Liverpool; University of London, Imperial College of Science, Technology and Medicine; University of London, Queen Mary and Westfield College; University of London, Royal Holloway and Bedford New College; University of Manchester; University of Massachusetts; University of Mississippi; Mount Holyoke College; University of Notre Dame; Rutherford Appleton Laboratory; Shanghai Institute of Ceramics; Stanford Linear Accelerator Center.

1. The BABAR Collaboration, BABAR Technical Design Report, SLAC-R-95-457, March 1995.
2. The Calorimeter Calibration Task Force, "Use of Radioactive Photon Sources with the BABAR Electromagnetic Calorimeters," BABAR Note 322 (1996).
3. The BABAR CsI Calorimeter Group, "Material for Preliminary Design Review," December 1996, unpublished.